A two-scale probabilistic time-dependent fatigue model for offshore steel wind turbines

Benjamin Rocher, Franck Schoefs, M.L.M. François, Arnaud Salou, Anne-Laure Caouissin

A two-scale probabilistic time-dependent fatigue model for offshore steel wind turbines

Benjamin Rocher

Université de Nantes, GeM, UMR CNRS 6183. Atlantique Engineering Solutions, Saint-Nazaire, France

Franck Schoefs

University de Nantes, Institute for Research in Civil and Mechanical Engineering (GeM), UMR CNRS 6183, Sea and Littoral research Institute - FR CNRS 3473, Nantes, France

Marc François

University de Nantes, Institute for Research in Civil and Mechanical Engineering (GeM), UMR CNRS 6183, Nantes, France

Arnaud Salou

Atlantique Engineering Solutions, Saint-Nazaire, France

Anne-Laure Caouissin

Atlantique Engineering Solutions, Saint-Nazaire, France

ABSTRACT

Due to both wave and wind fluctuations, the steel foundations of offshore wind turbines are highly submitted to fatigue. To date, current methods of fatigue design proposed in the regulations are not devoted to structural optimization and to the consideration of time-variant hazards. We propose hence an incremental two-scale model of damage in order to follow the time evolution of the damage. This temporal evolution allows the updating of model parameters using records from Structural Health Monitoring. In this paper, we focus on Bayesian updating of damage parameters and sensitivity analysis of damage assessment to material parameters.

Key words: damage model, reliability, fatigue, weld, offshore

1. INTRODUCTION

Design of foundations of offshore wind turbines (OWT) is quite different from that encountered for offshore Oil and Gas platforms. The great number of foundations in a wind farm requires adapted methods for design and maintenance; this contrasts with the prototype character of offshore platforms in Oil and Gas industry. Offshore steel trussed-shaped structures, called Jacket structures are the most popular bottom fixed one for supporting oil and gaz platforms and offshore wind substation. This paper focusses on them. They are built by welding cylindrical beams that form a lattice-like structure. The economic context of profitability of electric energy in the context of competition between sources (sun, coal, nuclear…) requires manufacturers to optimize their foundations: the objective is to reduce production costs to reduce the Levelized Cost Of Energy. This requires a low number of structural elements for building the frame, which implies less redundancy leading to a lower safety margin in the design. That is consistent with risk analysis because human and ecological consequences are lower than in Oil and Gas industry. Three limit states are checked: ultimate, fatigue and accidental situations. Fatigue Limit State (FLS) is one the most complex due to the uncertainties both in loading and resistance and relies on simplistic assumptions.

Due to its large scatter, marine environment is modelled as a stochastic input for the design. Some statistics about wind speed and direction, wave height, period and direction, *etc*. are available. Other uncertainties occur: structural uncertainties caused by manufacturing of welded joints (Pasqualini et al., 2013, Schoefs et al., 2016) and uncertainties in resistance (fatigue curves). Due to these uncertainties, many design approaches exist. Some of them used partial security factors but they often produce a conservative design of structure. Reliability design based on uncertainties propagation through a structural model offers more flexibility for accounting for uncertainties and optimize the design, thus reducing the design costs. This paper focuses on the structural (geometry of welded joints) and material (material properties of welded area) uncertainties.

After briefly summarizing fatigue methods, we propose an incremental damage computation approach before crack initiation. This choice can limit the risk of large open cracks that cause a decrease of stiffness (Schoefs et al., 2008) and even the loss of structural elements in a preventive approach of the maintenance in link with continuous real-time Structural Health Monitoring. There is no tool at this time for assessing directly and accurately the damage. That is the reason why our objective is to combine the measurement of the stain with usual strain-sensors (electrical gauges or Fiber Optical Sensors) and to compute the damage from these measurements; it can be seen as a virtual damage sensor (VDS). This VDS is a hybrid sensor that couples a strain sensor and a damage computation.

This approach contrasts with current design rules where times of crack initiation and failure are combined (DNV.GL, 2014). It differs also from some recent approaches of fatigue reliability which focus on crack propagation (Dong et al. 2012). A key idea is that the time of crack propagation in structures with low redundancy as defined by EN-19931-1 (2005) can be neglected in comparison with the initiation time.

Some of the uncertainties presented above can be continuously monitored on site: wave and wind parameters from dedicated measurement masts or equipment of structures (with a specific care on corrosion and local stress). For some of them, measurement is still a challenge: marine growth, or crack. If continuous monitoring is not available, expensive discrete inspections should be carried out. In that case, real-time preventive optimization is not affordable

This paper is a first step of a larger study about preventive maintenance based on structural health monitoring. The challenge is the ability to implement this method in a reliability design process of a complex structure. A second challenge is the implementation in an industrial context with acceptable computation time. Two locks need to be solved. The first one relates to the calibration of the model in a stochastic context from experimental tests. The second one is the reduction of time computation which is a disadvantage of the temporal method chosen. This last point is not discussed in this article and is addressed since 2017 in the project MUSCAS (MUlti SCAle Stochastic computation for MRE) of Université de Nantes, supported by WEAMEC (Region Pays de la Loire). Here, we focus on the first lock in a study of a steel structure called jacket consisting of welded tubes assemblies (Figure 2).

Section 2 reminds the uncertainties that should be accounted for. Section 3 reviews the state of the art of existing methods for fatigue analysis of offshore structures. Damage model and parameters are presented in section 4. Section 5 introduces the probabilistic framework with the *a priori* probabilistic modelling of random variables and Bayesian updating from probabilistic S-N curves. Finally, a sensitivity analysis is performed in section 6 in view to rank these random variables according to their effect on S-N curves.

2. IDENTIFICATION OF SOURCES OF UNCERTAINTIES IN A FATIGUE ANALYSIS

Uncertainties are usually assigned to categories (Ditlevsen, 1982). The first level of categories consists in distinguishing random (or aleatory) and epistemic uncertainties. Random uncertainties are also called intrinsic uncertainties. The second level distinguishes two types of epistemic uncertainties: measurement uncertainties and uncertainties due to insufficient knowledge (approximation of the reality trough a simplified model).

2.1. Random uncertainties (intrinsic)

These uncertainties are intrinsic to the phenomena and it is not possible to reduce the scatter whatever the research/industrial efforts. They are present at two levels in our study: (i) distribution of results of fatigue tests (Wöhler curve) cannot be reduced to a deterministic value; the uncertainty comes in particular from the imperfections in the steel production process. The microstructures of steel are different from a casting sheet or welding shape to another, for a given established quality control. Thus, for a given level of applied load, it will always remain a distribution of the number of cycles to failure. (ii) The second phenomenon concerns environmental data of wave and wind and also marine growth (Schoefs, 2008, Schoefs and Boukinda, 2010; Ameryoun et al., 2019). The uncertainty is especially present in the randomness of the sequence of heights, periods and directions of waves and in the succession of different speeds and directions of wind.

2.2. Epistemic uncertainties

Unlike random uncertainties, epistemic uncertainties (Dubois and Guyonnet, 2011) can be reduced by making more efforts (improving the quality of manufacture, weld shape, or measurement techniques, strain measurement, increasing the number of experimental trials ...). Even if it is impossible to restore the data distributions to deterministic values, it is possible to reduce the scatter.

Indeed, no model can perfectly represent reality because of underlying assumptions. We incorporate here uncertainty associated with two-scale damage model. As explained above, the parameters need to be identified to calibrate the model on experimental trials. These tests include epistemic uncertainties. For instance, the scatter of experimental results may be reduced by increasing the number of tests (statistical uncertainty) and by using sensors whose accuracy is higher (sensitivity of measurement).

Environmental data are also affected by epistemic uncertainties because of the precision of the measuring devices (satellite, anemometer ...) (Magnusson 2013). We can therefore improve knowledge of the phenomenon by accumulating on site records.

2.3. Material and structural uncertainties

For fatigue evaluation of welded structures, the Wöhler (or S-N) curve is built from fatigue tests on samples. The scatter of results (number of cycles until failure) include geometrical uncertainties, uncertainty on the welded process and uncertainty on material properties at the local scale after welding: we embrace all these sources of uncertainty in the terms Material and Structural uncertainties. It links the applied stress range to the number of cycles to failure in a log-log relation and is generally

associated to 50% probability of survival. In design rules, 97.7% is commonly used. This design curve integrates material uncertainty and uncertainties generated by unrepeatability of the welding process.

The Standards ARSMM (1985) and DNVGL (2014) define S-N curves. For an applied stress range $\Delta\sigma_i$, this distribution follows a normal distribution with a standard deviation of 0.2 from DNV-GL and of 0.275 from ARSMM. In the following, the DNV-GL value is retained. A 97.7% probability of survival is associated to S-N curves presented in DNV-GL. With these information, it is possible to generate random values of number of cycles to failure for a selected stress range. Corresponding "experimental" test results can be simulated (Figure 1). Note that in case of large cracks, effect of the crack geometry on the component geometrical properties (area of cross section …) should also be considered (Schoefs et al., 2008).

Figure 1: 50 simulated trials from S-N curve (DNV-GL)

3. FATIGUE ASSESSMENT: EXISTING APPROACHES

3.1. General principles of local stress computation

In offshore wind industry, the rule commonly used for fatigue design method is provided by DNV-GL (2014). It is based on the use of computation of vibration with finite elements models. This is a current modelling for a full jacket and is adapted to model the distribution of loads on the structure (Morison equation) (Morison, 1950).

This method relies first on the stresses resulting from the normal force and bending moments on which stress concentration factors are applied. The stress concentration factors are dependent on the geometrical properties of the tubes and the shape of their connection (Figure 2). The combination is based on empirical formulas commonly known as Efthymiou formulas (Efthymiou, 1988). This allows studying the fatigue level of a geometric discontinuity where high stress concentration occurs, with a simple beam model of the structure. This method can be viewed as a one-dimensional approach. The randomness arises from the behaviour law of the material and natural loads.

Figure 2: Stress computation points around the circumference of a welded tubular joint and Jacket structure realized by Atlantique Engineering Solutions for Alstom offshore prototype Haliade 150 (photo: courtesy of Bernard Biger)

3.2. State of the art of S-N approaches

For a stress range $\Delta\sigma_i$ and a stress concentration factor computed at each of the eight points regularly spaced along the weld (Figure 2-left), we can determine N_i. According to the Miner rule (Miner, 1945), the damage d_i for this range can be calculated knowing n_i, the actual number of cycles for a stress range $\Delta\sigma_i$: d=n_i/N_i. The fracture is supposed to occur when d=$\sum d_i$ reaches a critical value D_c here taken equal to 1.

Efforts that generate these stress ranges come mainly from two environmental phenomena, waves and wind. They can be presented in the form of spectrum or time series. Depending on the shape of the available data, the fatigue analysis can be of two types, spectral or temporal.

Spectral fatigue is most commonly used. However, it does not allow updating of random variables from continuous time monitoring and is therefore not suitable for Structural Health Monitoring (SHM): that is the case for corrosion, crack initiation, local stresses, marine growth measurements. These ones can be recorded during the service lifetime. In addition, many simplifying assumptions are made and can be widely questioned. For instance, effect of mean stress and, obviously, loading history are not accounted explicitly and the linear cumulative Miner's law of damage is said to be questionable too, especially in presence of complex sea-states as explained by Olagnon (Olagnon et al., 2014).

3.3. State of the art of fracture mechanics in reliability context

Another approach is also currently used to estimate remaining lifetime of jacket structures in the aim to optimize maintenance (Guedes Soares and Garbatov, 1998). Based on fracture mechanics, they proposed a study of maintained ship hull girders submitted to corrosion and fatigue in which they model parameters of crack propagation law as random variables.

Following this approach, Moan (Moan et al. 1999) presented applications for jacket structures of Oil and Gas platforms. These structures were generally designed with a high conservatism because of dramatic consequences in case of failure. They used crack propagation models because a loss of tubular member is not always critical in such redundant structures.

Dong (Dong et al. 2012) used this method in the case of jacket support structures for offshore wind turbines. They utilized this crack propagation approach based on Paris' law (1) because crack observation can easily be done by visual inspection and stiffness can be updated (Schoefs et al., 2008).

$$\frac{da}{dN} = C(\Delta K)^m \tag{1}$$

Where a is the crack depth, N is the number of stress cycles, C and m are material parameters and ΔK is the stress intensity factor range proposed by Newman and Raju (Newman Jr. and Raju, 1981). For fatigue failure, they used the safety margin presented in (2), for which a Weibull distribution of $\Delta\sigma$ is required.

$$M(t) = \int_{a_0}^{a_c} \frac{da}{\left(\gamma_Y Y \sqrt{\pi a}\right)^m} - C\nu_0(t - T_0)A^m\Gamma\left(1 + \frac{m}{B}\right) \quad (2)$$

Where a_0 is the initial crack size, a_c is the critical crack size, T_0 is the initiation period, ν_0 is number of stress cycles a year, Y is the geometry function multiplied by a random variable γ_Y. Safety margin form is $M = R - S$ where R is the resistance corresponding to the number of cycles during crack propagation from a_0 to a_c and S is the load corresponding to the number of cycles before time t. The safety margin we consider in the following writes: $M(t) = D(t) - D_c$, with D_c =1. The associated failure probability at any time t is defined by (3).

$$P_f(t) = P(M(t) < 0) \quad (3)$$

Authors (Dong et al. 2012) have shown the possibility to optimize operations and maintenances of jackets for OWT. But, in the field of OWT where design costs play a significant role on energy production cost, conservatism during design phase should be reduced: Jacket structures are less redundant than in oil and gas field. Thus, the approach proposed by Dong (Dong et al. 2012) becomes not adapted. This is why, this paper presents a new model of fatigue based on crack initiation approach. Indeed, it is estimated that no crack is acceptable.

4. PROPOSED MODEL

4.1. Two-scale damage model

We retained a fatigue analysis based on a two-scale damage model, originally proposed by Lemaitre (Lemaitre 1996), applied to fatigue by Lemaitre (Lemaitre, 1999; Lemaitre and Desmorat 2005) and applied to marine structures by Thevenet *et al.* (Thevenet et al., 2015). It postulates the existence of microscopic spherical inclusions in which the material properties are degraded. In these inclusions plasticity and damage occurs, while the surrounding material remains in elasticity. Quite recently, the assumption of weak domains proposed by Lemaitre has been justified by thermal imaging of the high cycle fatigue phenomenon (Chrysochoos and Louche 1998, 2000). It was observed during

a test of monotonic loading that the heat sources, which reveal dissipative behaviour (plasticity or damage), are located only at some points and not everywhere.

The model is used here for welded areas (Figure 2), commonly identified as crack apparition areas. Following the rules of conception (DNV-GL, 2014), the tensile stress in the weld, associated with the mode 1 crack opening, is calculated (at eight points) as a linear combination of the normal force and flexural momentums given by a beam model of the whole structure. Dealing only with this tensile stress, the damage model, initially in 3D, is used here in its 1D version.

The surrounding sound material remains in elasticity during the cyclic loading: $\sigma = E\varepsilon$ where the macroscopic stress σ ranges from $-\sigma_a$ to σ_a, with $|\sigma| < \sigma_y$, the macroscopic limit of elasticity, and where E is the Young's modulus and ε the macroscopic strain. On the contrary, the microscopic inclusion, denoted by μ, possesses a yield stress σ_y^μ smaller than σ_y thus cycles show plastic evolutions B'A and A'B during which damage occurs (Figure 3).

Figure 3: Two-scale model scheme (left) and response to a symmetric cycle (right).

The effect of damage is to diminish both the apparent Young's modulus and the stress level. Following the damage theory, the Hooke law in the inclusion is $\tilde{\sigma}^\mu = E(\varepsilon^\mu - \varepsilon^{\mu p})$ where $\varepsilon^{\mu p}$ is the plastic strain, $\varepsilon^{\mu e} = \varepsilon^\mu - \varepsilon^{\mu p}$ the elastic part of the strain, $\tilde{\sigma}^\mu = \sigma^\mu/(1-D)$ the effective stress and $D \in [0,1]$ the damage level. According to the Lin-Taylor localization rule, the microscopic strain ε^μ is always equal to the macroscopic strain ε.

For sake of simplicity, the plasticity is supposed to be of the linear kinematic hardening type with a Von-Mises type yield surface:

$$f(\tilde{\sigma}^\mu, X^\mu) = |\tilde{\sigma}^\mu - X^\mu| - \sigma_y^\mu \qquad (4)$$

Where $X^\mu = \frac{2}{3}C(1-D)\varepsilon^{\mu p}$ is the back stress, proportional to the plastic strain $\varepsilon^{\mu p}$ *via* the hardening modulus C. The damage is supposed isotropic and to evolve as:

$$dD = \left(\frac{Y}{S}\right)^s H(p - p_d)dp \qquad (5)$$

Where $Y = (\tilde{\sigma}^\mu)^2 2E$ is the release rate of elastic energy, S and s are material parameters and *p*, defined by $dp = |d\varepsilon^{\mu p}|$ is the cumulated plastic strain. The fatigue damage starts when p reaches a

threshold p_d, as indicated by the Heaviside function H and increases up to the critical damage D_C at which the crack initiation takes place supposed, in our approach, to lead instantaneously to failure.

Figure 4 gives the flowchart of the two scales computation.

Figure 4: Flowchart of the two scales damage computation

An analytical resolution (Appendix 10.1) gives the number of cycles at the beginning of damage N_D and the number of cycles leading to failure N_R. These expressions summarize as $N_R = M_{an}(Z, \epsilon)$ where-$Z = \{C, S, s, {\sigma_y}^{\mu}, p_d, D_C\}$ is the vector material parameters.

Figure 5 shows the link between the applied stress range and the number of cycles to failure. S-N curves associated to 97.7% probability of survival is presented in (DNV-GL, 2014). Equations of the two-scales model have been used with a manual calibration of the parameters in order to fit the 97.7% curve. Figure 5 shows the good agreement between N_R and the reference S-N curve, except for the rounding at the intersection of the two straight lines. However, experimental S-N curves do present such rounding and the damage model has this capacity.

Figure 5: S-N curve from (Det Norske Veritas and Germanischer Lloyd 2014)

The computation time for identification is a major issue in the case of SHM where the model will be extended to a numerical model involving a calculation of complete structure (in particular the structural node). It is therefore important to limit the size of our probabilistic space. To this end, we propose, in a first step, a Bayesian updating of random variable distributions and then a sensitivity analysis by elasticity (in the statistical sense). Indeed, we do not have prior distributions of the parameters in the literature. Only the variation ranges are known and will help as limits of prior uniform distributions.

5. PROBABILISTIC MODELLING AND BAYESIAN UPDATING

In this section, the objective is to provide probability density functions for each basic random variable. From the literature, we determine a prior distribution of the two-scale model parameters from the bounds given by Lemaitre (Lemaitre and Desmorat 2005; Lemaitre 1996). We propose a Bayesian updating of these distributions based on simulated trials from S-N curve presented in (DNV-GL, 2014).

5.1. Probabilistic modelling

Before updating, prior key steps of a probabilistic mechanical problem should be followed:

- Identification of the basic variables.

- Choice of marginal distributions.
- Dependence between variables (co-moments ...).

Elastic modulus E is commonly considered as a deterministic parameter because of its low coefficient of variation (around 5%) in comparison with others. The parameter s has a major impact on S-N curve shape. Tests revealed that, as suggested by Lemaitre himself, the best value of s should be 1. s is hence considered as a deterministic parameter. Finally, $\sigma_y{}^{\mu}$ is deterministic because it can be easily identified on a S-N curve as the fatigue limit at 10^6 cycles.

Thus, we choose Z=(S, p_d, D_C) as the vector of random variables with associated uniform distributions. The choice of a uniform prior distribution includes a non-informative aspect unlike to normal or lognormal distributions for example. This non-informative prior distribution is usually introduced when the properties of the material are unknown (for instance after a complex degradation process), when no direct measurement of a parameter is available or when no probabilistic modelling or statistical analysis was carried out until now: this study in the latter case. A literature review has identified some values of the model parameters. This therefore gives a first assumption on their range of possible variation. The values found were not obtained for steel strictly identical to the present study; that is why the range of variation was extended. Also, no assumption on the correlation between random variables is considered. We are aware that this assumption is strong but at this stage of our study and from expert judgement, no other assumption can be stated.

Table 1: Parameters ranges of variation

5.2. Bayesian updating by MCMC

When statistics of condition state measurements are obtained from inspection of a structural component and when some prior knowledge is available from a model, it is interesting to compare them. Differences are observed. In order to optimize future predictions, it is interesting to update the input parameters of the degradation model taking into account inspections or measurements. To this end, we decide to use Bayesian updating combined with the variability of input parameters (Dubourg, 2011). Bayesian updating is an application of the continuous formulation of Bayes theorem. Measurements are samples (simulated trials) from the probabilistic distribution of S-N curves.

Bayesian updating used in this study is based on Monte-Carlo Markov Chains Markov (MCMC) (Perrin, 2008). We carry out this method based on S-N curves and their distribution from DNV-GL (DNV-GL, 2014). Realizations are plotted on Figure 5. We focus on material parameters updating of Z from analytical model $M_{an}(Z, \epsilon)$ outputs (Berveiller et al. 2007, 2008).

5.2.1. Bayes theorem

Let $p_Z(z)$ be the *a priori* multidimensional probability density (prior distribution) of Z. This function can be estimated from experimental data or expert judgment. Due to lack of information, uniform distributions are used to described prior probability density $p_Z(z)$. Let Y^{obs} *(6)* be a set of available observations used for updating.

$$Y^{obs} = \{y(z_p); p = 1, \dots, P\} \tag{6}$$

The observations are realizations of the random vector Z. Thus, Bayes' theorem gives the posterior probability density $f_Z(z)$ of the random vector Z by:

$$f_X(x) = \frac{1}{c} p_Z(z) L(z, Y^{obs}) \tag{7}$$

$L(z, Y^{obs})$ is the likelihood of the observations and c is a normalization constant used to define the probability density function $f_Z(z)$.

5.2.2. Updating method

Distribution of experimental observations and of model outputs are different. Thus, an approximation error of model outputs, called E**,** exists. Error and observation variable have the same expression because a realization $e(z_p)$ of error E corresponds to an observation *(8)***.** We commonly consider that the error follows a normal distribution with a standard deviation σ_e.

$$E = \{e(z_p); p = 1, \dots, P\} \tag{8}$$

Each observation can be written as a function of model $M_{an}(Z)$ and the realization of the model error E (9).

$$y(z_p) = M_{an}(Z) + e(z_p) \tag{9}$$

Knowing the parametric form of the prediction model $M_{an}(Z)$ and assuming that observations are independents, the likelihood of the observations can be written:

$$L(z, Y^{obs}) = \prod_{p=1}^{P} \varphi\left(\frac{M_{an}(z) - y(z_p)}{\sigma_e}\right) \tag{10}$$

Where φ is density function of the standardized (zero mean and standard deviation 1) normal random variable. Thus, posterior distributions of the input parameters follow the pdf in (11).

$$f_{Z,\sigma}(z,\sigma) = \frac{1}{c} p_Z(z) p_{\sigma_e}(\sigma_e) \prod_{p=1}^{P} \varphi\left(\frac{M_{an}(z) - y(z_p)}{\sigma_e}\right) \quad (11)$$

In this study, prior probability density function of each variable is a uniform distribution defined on variation range identified from literature (section 5). The value of c is obtained from equation (12).

$$\frac{1}{c} = \int_{R^{n_Z}} p_Z(z) \prod_{p=1}^{P} \varphi\left(\frac{M_{an}(z) - y(z_p)}{\sigma_e}\right) dz \quad (12)$$

Where n_Z corresponds to dimension of vector Z (here n_Z = 3).

Monte-Carlo methods by Markov chains (MCMC) are numerical technics, which let to simulate posterior probability density function of Z without evaluating equation (12). Only likelihood function and prior probability density function $p_Z(z)$ of Z are needed. The MCMC procedure is solved using a sequential Metropolis-Hastings algorithm (Hastings 1970; Metropolis and Ulam 1949). The algorithm selected in this paper is the version published by (Tarantola, 2005).

5.2.3. Model error definition

Error function used in MCMC algorithm has to be correctly defined. It means that all the measurements shall be compared with the different simulations. It depends on available measurements and model variability created by a new set of parameters. Natural expression of error function is:

$$e_{ij} = N_{exp_i} - N_{model} \quad (13)$$

Thus, the associated likelihood function is:

$$L = \prod_{j}^{m} \prod_{i}^{n} \varphi(e_{ij}) \quad (14)$$

Where n is the number of available measurements for stress range $\Delta\sigma_j$ and m is the number of stress ranges in the samples of simulated trials.

With equation (13), error value evaluated for two levels of stress ranges $\Delta\sigma_j$ can be different with a factor 1000. Convergence of the algorithm is easier to ensure by reducing the biggest error. That is why MCMC algorithm correctly estimate the number of cycles associated with the lowest stress range $\Delta\sigma_j$ because this is where error value is the most important. Fatigue updating from S-N curves is very sensitive to this shortcoming since the scatter of N_R is large.

Table 2 presents four others expressions of error function in order to avoid this phenomenon.

Table 2: Error and likelihood functions

The number of observations P presented in (6) depends on error expression. $P = m$ for functions 2 to 4 and $P = m \times n$ for function 1.

5.3. Results

Due to error expression of Function 1 and a great number of observations, associated likelihood value is nearly null and close to the numerical accuracy of software. This is a problem for MCMC convergence. Thus, Function 1 cannot be chosen. Function 2 produces model outputs closed to S-N curve associated to 50% probability of survival. But, in a design process, it is important to correctly estimate distributions tails, especially the one of the low numbers of cycles. In this case, Function 4 produces better results than other functions and is presented in Figure 6. Black dots represent the simulated trials used for the MCMC and grey dots represent results of simulations from identified parameters.

Figure 6: Superposition of number of cycles distribution and of S-N curves

5.3.1. Crude marginal distributions

Figure 7 shows the posterior distributions of two parameters; others are available in Appendix 10.2. Distribution of D_C is non-symmetric which already provides a first level of information about the probabilistic modelling of this variable (Weibull, Lognormal, etc.).

Figure 7: Superposition of uniform prior distribution and discrete posterior distribution (C on the left and D_C on the right)

After identification, coefficients of variation (CoV) calculated from discrete posterior distributions are given in Table 3 with acceptation levels of parameters. Coefficients of variation are quite low and acceptation levels are high enough. Thus, we can estimate that the model is correctly calibrated in a stochastic context.

Table 3: Coefficients of variation and acceptation levels

5.3.2. Correlation between input variables

Linear correlation coefficients are determined after Bayesian updating (Table 4). They show that parameters are mainly independent.

Table 4: Linear correlation coefficients

Nevertheless, S-D_c couple has a linear correlation coefficient greater than the others. It can be explained quite easily. Two phases are identified during fatigue test. The first one is before damage initiation: only C and p_D impact the number of cycles associated with this phase. Thus, when C is fixed, only S and D_C can be used to adjust model with observations. Relation between S and D_C is observed in the scatter diagram presented in Figure 8; others are available in Appendix 10.3.

Figure 8: Correlation diagram of D_C and S

6. SENSITIVITY ANALYSIS

A first sensitivity analysis by elasticity method is realized from the analytical expression of the model using ranges of variation and associated uniform prior distribution of the parameters. A second sensitivity analysis is done using results from the Bayesian updating.

6.1. Analytical expressions for sensitivity analysis

Following the approach suggested in (Schoefs, 2008) for monotonic models, we realize a first order Taylor expansion (15) of (*A10*) in Appendix 10.1 around the mean values, which determines the relative sensibility $\delta N_R/N_R$ of N_R from the logarithmic derivatives of (*A10*).

$$\frac{\delta N_R}{N_R} = \sum_k S_{A_k}^{N_R} \frac{\delta A_k}{A_k} \tag{15}$$

With $S_{A_k}^{N_R}$, the weight associated with the parameter A_k.

We present for example in (16) the expression of the weight associated with parameter C. Expressions of other parameters are summarized in Appendix (section 10.4).

$$\begin{aligned} S_C^{N_R} = {} & \frac{N_D}{N_R}\frac{2C}{2C+3E} \\ & + \frac{N_R - N_D}{N_R}\left(1\right. \\ & \left. + \frac{(2s+1)\sigma_a^{\mu}\left(\left(\sigma_a^{\mu}\right)^{2s} + \left(2\sigma_y^{\mu} - \sigma_a^{\mu}\right)^{2s}\right)}{\left(\sigma_a^{\mu}\right)^{2s+1} - \left(2\sigma_y^{\mu} - \sigma_a^{\mu}\right)^{2s+1}} \frac{8C^2\sigma_a + 6EC\left(\sigma_a + \sigma_y^{\mu}\right)}{\left(2C\sigma_a + 3E\sigma_y^{\mu}\right)(2C+3E)}\right) \end{aligned} \tag{16}$$

N_D and N_R are estimated from σ_a and mean values of the parameters.

In the case of monotonic regular perturbation around the mean values, the sensitivity can also be expanded as:

$$\frac{\delta A_k}{A_k} \cong \frac{\Delta A_k}{A_k} \tag{17}$$

6.2. *Results of the sensitivity analysis*

6.2.1. *Before Bayesian updating*

The sensitivity analysis by elasticity is achieved using the mean values of variation ranges of each model parameter and its coefficient of variation. Information about parameter are summarized in Table 5.

Table 5: Ranges of variation, means and coefficient of variation of parameters before Bayesian updating

Figure 9 plots the sensitivity to each variable in the SN.

Figure 9: Sensitivity indexes in % (prior)

There is a disparity in variables weight. This analysis shows that the most influential variables are C, S and D_C. S and D_C have nearly the same weight because they play together in order to adjust model response (see 5.3.2).

6.2.2. *After Bayesian updating*

A second sensitivity analysis is realized after the Bayesian updating. Here, mean values of the parameters do not correspond with central values of variation ranges (Table 6). Results are presented in Figure 10 as a function of the stress range.

Table 6: Ranges of variation, means and coefficient of variation of parameters after Bayesian updating

Figure 10: Sensitivity indexes in % (posterior)

Parameters weights are not really different except for low ranges ($\text{Log}(\Delta\sigma)<5.10^2$). The same conclusion can be done. Curve represented from mean value of the parameters is interesting. Indeed, this curve shows that mean value of the parameters let to fit correctly with S-N curve at 50% probability of survival.

7. CONCLUSION

Fatigue reliability assessment in the time-domain is the most promising way for introducing Structural Health Monitoring in a risk analysis. That is required for optimizing operation and maintenance, by defining the optimal time of repair or detailed inspection.

We can cite many advantages of this modelling we consider as essential, such as:

- The time evolution of the damage which is essential for SHM and the consideration of historical loading;
- The taking into account of all components of the stress tensor including the effect of mean stress;

However, it presents two major drawbacks. The first one concerns the computation time which can be significant if a strategy is not implemented. The second one concerns the model for which it is necessary to lead a calibration over experimental tests by playing with the influential parameters. The paper faces this latter objective. The whole process of fatigue design faces the presence of uncertainties. It is important to be able to identify, quantify and spread them for assessing the lifetime.

This goal requires a probabilistic model of damage propagation. The paper first reminds the two-scale damage model that includes 6 parameters. Another requirement is to use as much as possible the existing data, especially SN-curves that required huge experimental efforts during the four past decades. It is shown that the two-scale damage model fit well these SN-curves, including their lower limit.

Finally, the paper considers the random SN-curves and fit the joint distribution of parameters after a specific development of the error function for the MCMC algorithm. A sensitivity analysis shows that:

- only four variables play a dominant role and that the two others can be modelled as deterministic parameters;
- the relative influence of these 4 variables depends of the level of stress;
- some parameters are correlated and should be modelled as such when propagated for reliability assessment.

This paper is the basis for future researches: reliability assessment and damage updating from Structural Health Monitoring of strains.

8. ACKOWLEDGMENTS

The authors acknowledge the Région Pays de la Loire for supporting the SURFFEOL project (2014-2018), leaded by Chantiers de l'Atlantique.

9. REFERENCES

Ameryoun A., Schoefs F., Barillé L. Thomas Y. (2019). "Stochastic modeling of forces on jacket-type offshore structures colonized by marine growth". *Journal of Marine Science and Engineering, section Ocean Engineering, Marine Structures*, 7(5)/(may 2019), #158, https://doi.org/10.3390/jmse7050158.

ARSMM (Association de Recherche sur les Structures Métalliques Marines). (1985). *Assemblages tubulaires soudés. Guides Pratiques sur les Ouvrages en Mer*, Paris.

Berveiller, M., Pape, Y. Le, and Sudret, B. (2007). "Bayesian updating of the long-term creep strains in concrete containment vessels using a non intrusive stochastic finite element method.". *International Conference on Applications of Statistics and Probability in Civil Engineering (ICASP)* – Kanda, Takada & Furuta (eds) 2007 Taylor & Francis Group, London, ISBN 978-0-415-45211-3, 1–8.

Berveiller, M., Le Pape, Y., Sudret, B., and Perrin, F. (2008). "Méthode MCMC pour l'actualisation bayésienne des déformations différées du béton d'une enceinte de confinement modélisée par éléments finis stochastiques non intrusifs." *Journées Fiabilité des Matériaux et des Structures*, Nantes.

Chrysochoos, A., and Louche, H. (1998). "Analyse thermographique des mécanismes de localisation dans des aciers doux." *Comptes Rendus de l'Académie des Sciences - Series IIB - Mechanics-Physics-Chemistry-Astronomy*, 326(6), 345–352.

Chrysochoos, A., and Louche, H. (2000). "An infrared image processing to analyse the calorific effects accompanying strain localisation." *International Journal of Engineering Science*, 38(16), 1759–1788.

Ditlevsen, O. (1982). "Model uncertainty in structural reliability". *Struct Safety* 1982;1(1):73–86

DNV.GL (Det Norske Veritas and Germanischer Lloyd) (2014). *RP-C203 : Fatigue design of offshore steel structures*. Recommanded Practice, Edition DNV GL, AS April 2016.

Dong, W., Moan, T., and Gao, Z. (2012). "Fatigue reliability analysis of the jacket support structure for offshore wind turbine considering the effect of corrosion and inspection." *Reliability Engineering &*

System Safety, Elsevier, 106, 11–27.

Dubois, D. and Guyonnet, D. (2011). "Risk-informed decision-making in the presence of epistemic uncertainty". *International Journal of General Systems*, 40:2, 145-167, DOI: 10.1080/03081079.2010.506179

Dubourg, V. (2011). “Adaptive surrogate models for reliability analysis and reliability-based design optimization.” PhD Thesis, Université Blaise Pascal - Clermont-Ferrand II.

Efthymiou, M. (1988). Development of SCF formulae and generalized influence functions for use in fatigue analysis, *Recent Developments in Tubular Joint Technology*, OTJ'88, October 1988, London.

EN 1993-1-1 (2005). "Eurocode 3: Design of steel structures - Part 1-1: General rules and rules for buildings". Authority: The European Union Per Regulation 305/2011, Directive 98/34/EC, Directive 2004/18/EC.

Guedes Soares, C., and Garbatov, Y. (1998). “Reliability of maintained ship hull girders subjected to corrosion and fatigue.” *Structural Safety*. 20:3, Sept. 1998, 201-219.

Hastings, W. (1970). “Monte Carlo sampling methods using Markov chains and their applications.” *Biometrika*, 57(1), 97–109.

Lemaitre, J. (1996). *A Course on Damage Mechanics*. Springer-Verlag Berlin Heidelberg 1996. Second Revised and Enlarged Edition.. ISBN 978-3-540-60980-3.

Lemaitre, J. (1999). “A two scale damage concept applied to fatigue”. International Journal of Fracture, 97, 67-81.

Lemaitre, J., and Desmorat, R. (2005). *Engineering Damage Mechanics*. *Springer-Verlag Berlin Heidelberg 2005, ISBN 978-3-540-21503-5*.

Magnusson, A. K. (2013). “Variability of sea state measurements and sensor dependence". *Workshop: Statistical models of the Metocean environment for engineering uses,* IFREMER 30.09 01.10.2013.

Metropolis, N., and Ulam, S. (1949). “The Monte Carlo method.” *Journal of the American Statistical Association*, 44(247), 335–341.

Miner, M.A. (1945): "Cumulative Damage in Fatigue". *Journal of Applied Mechanics*, 67, A159.

Moan, T., Johannesen, J. M., and Vårdal, O. T. (1999). “Probabilistic Inspection Planning of Jacket Structures.” Offshore Technology Conference.

Morison, J. R.; O'Brien, M. P.; Johnson, J. W.; Schaaf, S. A. (1950). "The force exerted by surface

waves on piles". P*etroleum Transactions, American Institute of Mining Engineers,* 189: 149–154, doi:10.2118/950149-G

Newman Jr., J. C., and Raju, I. S. (1981). “An empirical stress-intensity factor equation for the surface crack.” *Engineering Fracture Mechanics*, 15(1–2), 185–192.

Olagnon, M., Kpogo-Nuwoklo, K.A. and Guédé, Z. (2014). " Statistical processing of West Africa wave directional spectra time-series into a climatology of swell events". *Journal of Marine Systems,* 130(Feb 2014), 101-108, https://doi.org/10.1016/j.jmarsys.2013.07.003.

Pasqualini O., Schoefs F., Chevreuil M., Cazuguel M.,(2013). ”Measurements and statistical analysis of fillet welded joints geometrical parameters for probabilistic modelling of the fatigue capacity”, *Marine Structures*, 34/dec. 2013, 226-248, doi: 10.1016/j.marstruc.2013.10.002 – 201

Perrin, F. (2008). “Prise en compte des données expérimentales dans les modèles probabilistes pour la prévision de la durée de vie des structures.” PhD Thesis, Université Blaise Pascal, Clermont Ferrand.

Schoefs, F. (2008). “Sensitivity approach for modelling the environmental loading of marine structures through a matrix response surface.” Reliability Engineering & System Safety, 93(7), 1004–1017,, doi: dx.doi.org/10.1016/j.ress.2007.05.006

Schoefs, F., Le Van, A., Rguig, M. (2008). “A Cracked Finite Element for Through-Cracked Tube”, Communications in Numerical Methods in Engineering, Published Online 6 March 2007, Vol. 24, 761-775, doi.wiley.com/10.1002/cnm.988

Schoefs F., Boukinda M.L. (2010). ”Sensitivity Approach for Modelling Stochastic Field of Keulegan Carpenter and Reynolds Number Through a Matrix Response Surface”. Journal of Offshore Mechanics and Arctic Engineering (JOMAE), section ‘Safety and Reliability’, 132:1/Feb. 2010, 1-7, doi: dx.doi.org/10.1115/1.3160386, 2010

Schoefs F., Chevreuil M., Pasqualini O., Cazuguel M. (2016). “Partial Safety Factor Calibration from Stochastic Finite Element Computation of Welding Joints with Random Geometries”, *Reliability Engineering and System Safety*, 155:NOV 2016, 44–54; doi: 10.1016/j.ress.2016.05.016

Tarantola, A. (2005). *Inverse Problem Theory and Methods for Model Parameter Estimation*. *Society for Industrial and Applied Mathematics (SIAM)*, series 'Other Titles in Applied Mathematics'.

Thevenet, D., Erny, C., Cognard, J.Y. and Korner, M. (2009). « Modélisation du comportement en fatigue d’assemblages soudés de type naval », 19ème Congrès Français de Mécanique. Marseille.

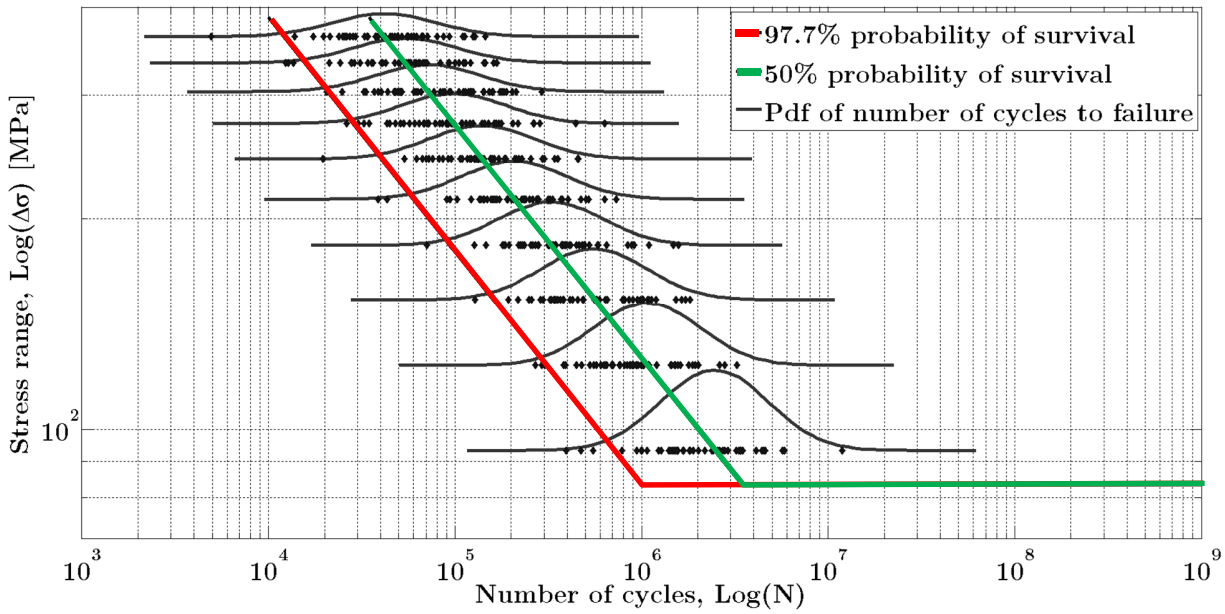

Figure 1: 50 simulated trials from S-N curve (DNV-GL)

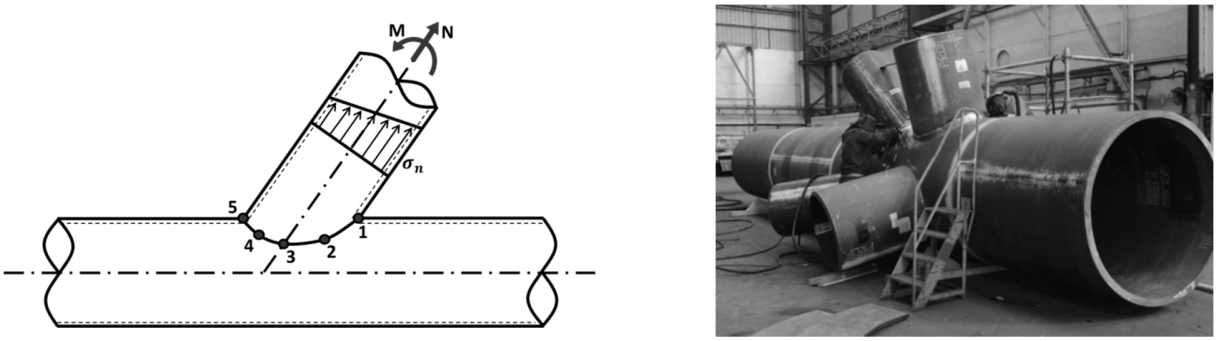

Figure 2: Stress computation points around the circumference of a welded tubular joint and Jacket structure realized by Atlantique Engineering Solutions for Alstom offshore prototype Haliade 150 (photo courtesy of Bernard Biger)

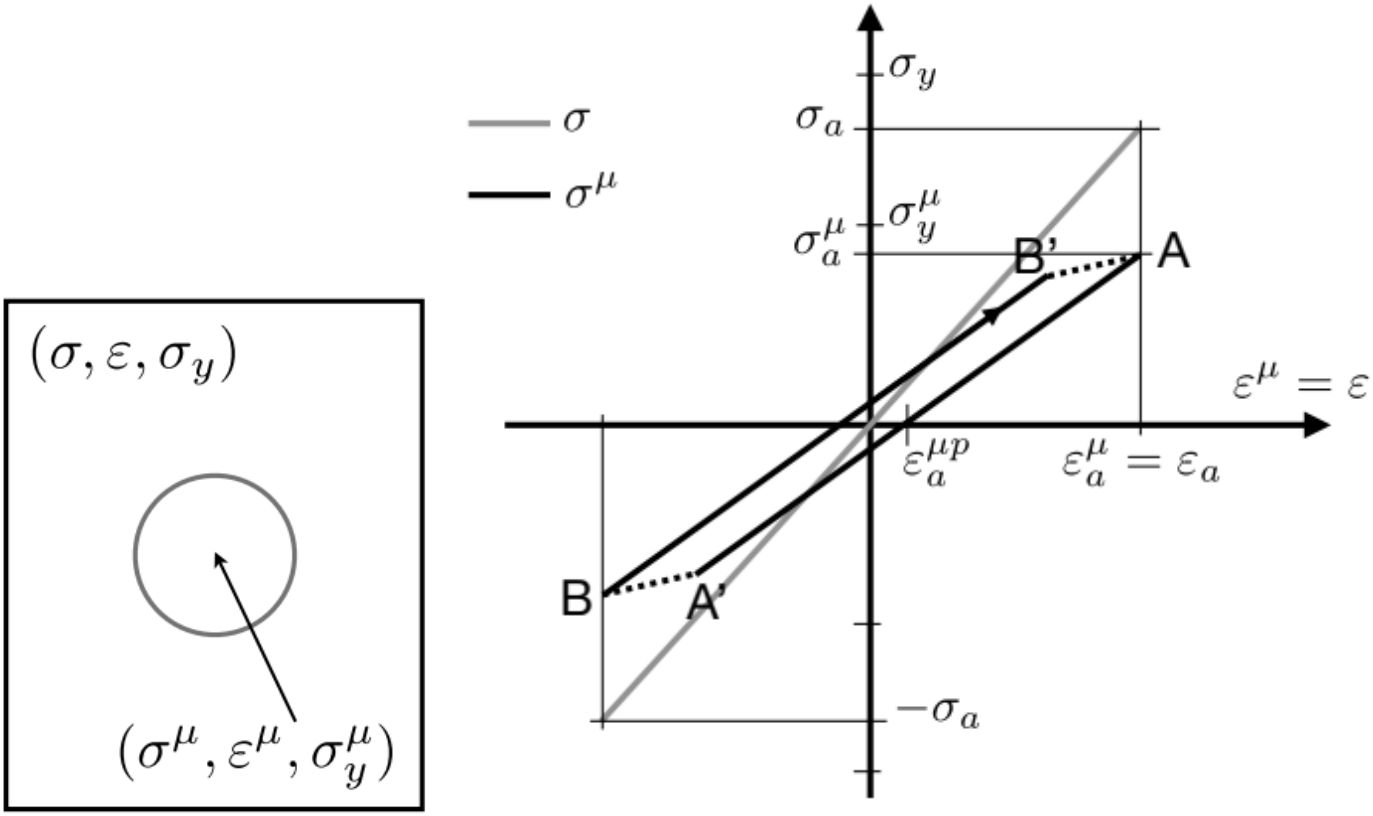

Figure 3: Two-scale model scheme (left) and response to a symmetric cycle (right)

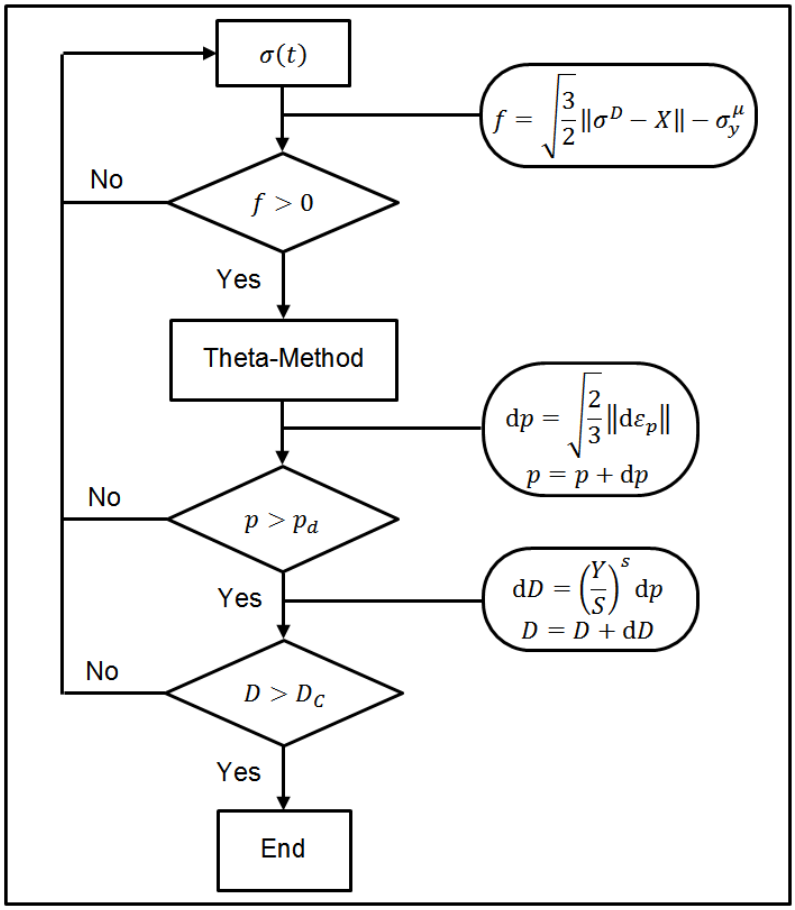

Figure 4: Flowchart of the two scales damage computation

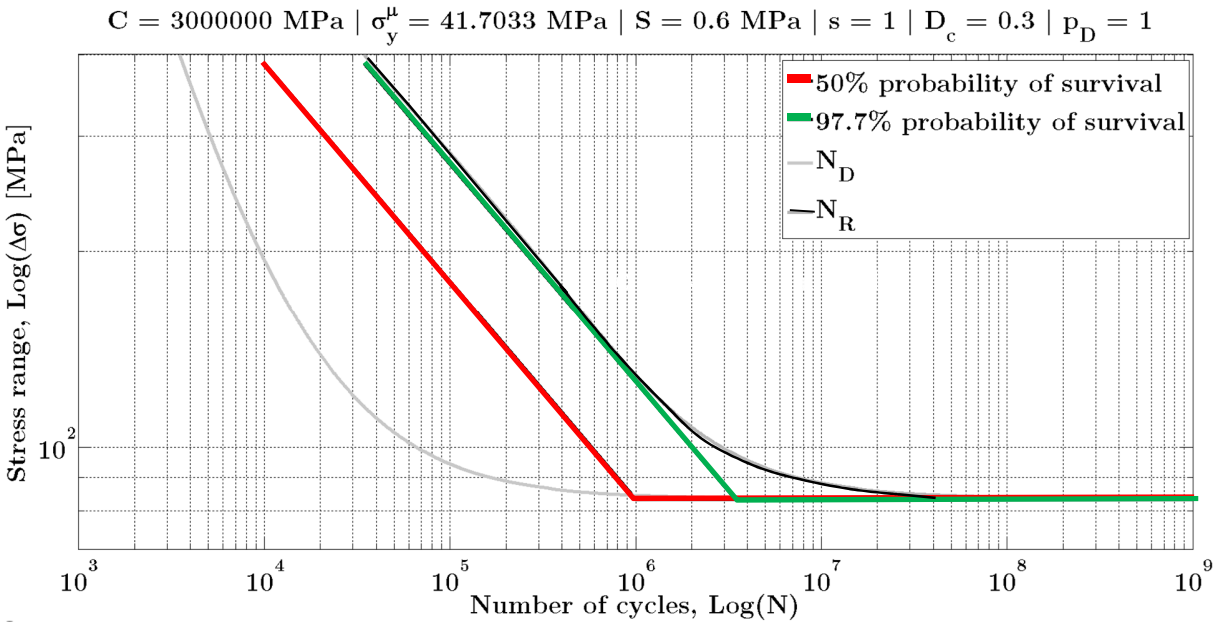

Figure 5: S-N curve from (Det Norske Veritas and Germanischer Lloyd 2014)

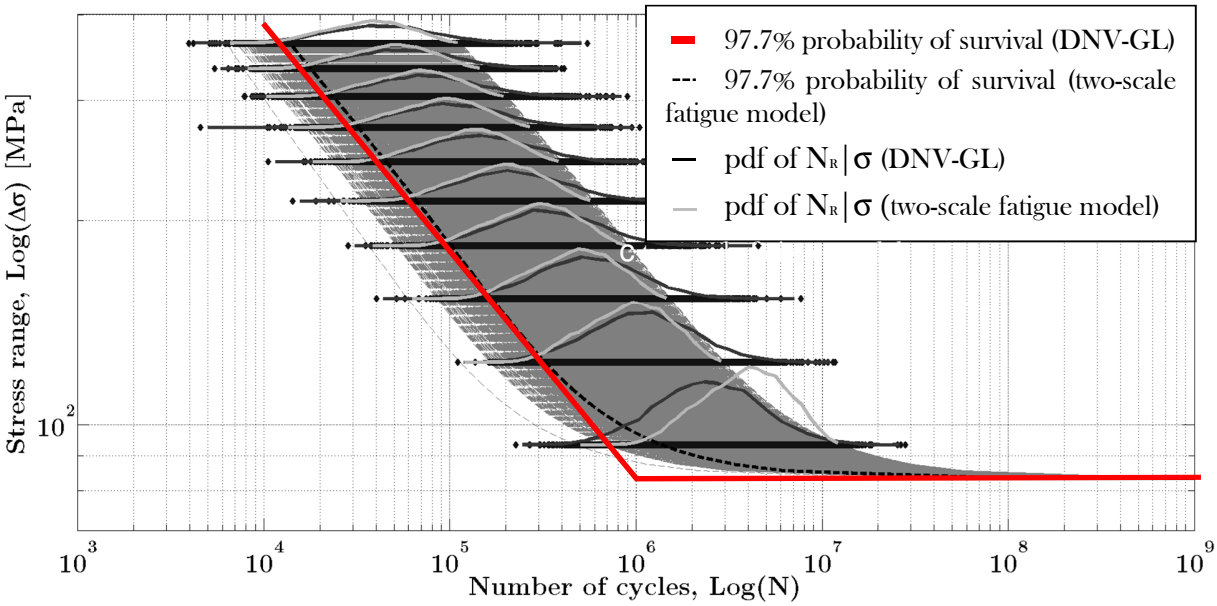

Figure 6: Superposition of number of cycles distribution and of S-N curves

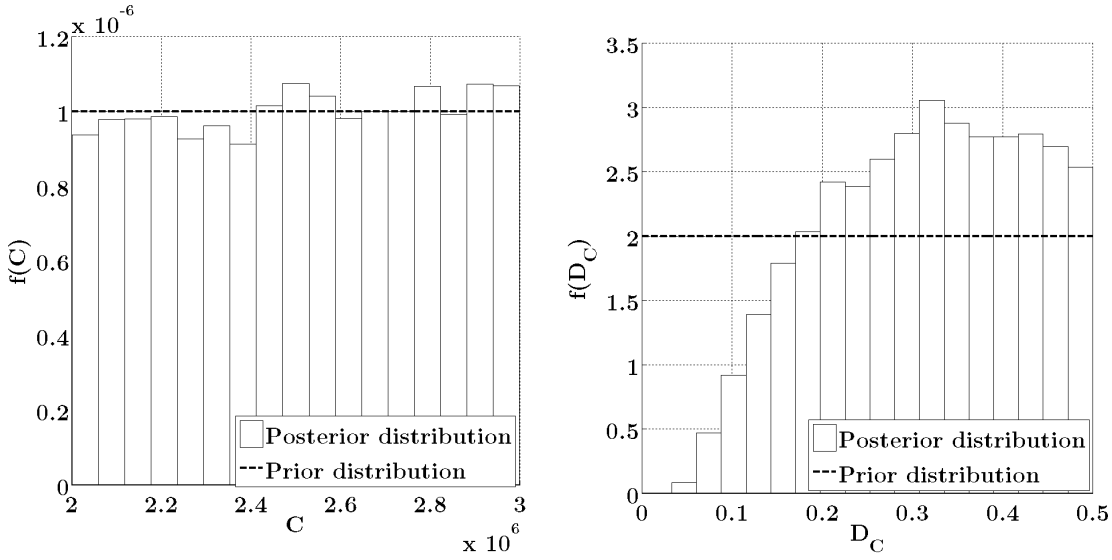

Figure 7: Superposition of uniform prior distribution and discrete posterior distribution (C on the left and D_C on the right)

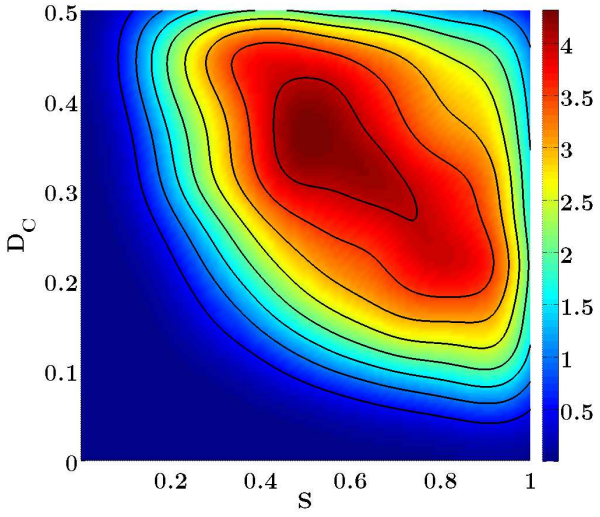

Figure 8: Correlation diagram of D_C and S

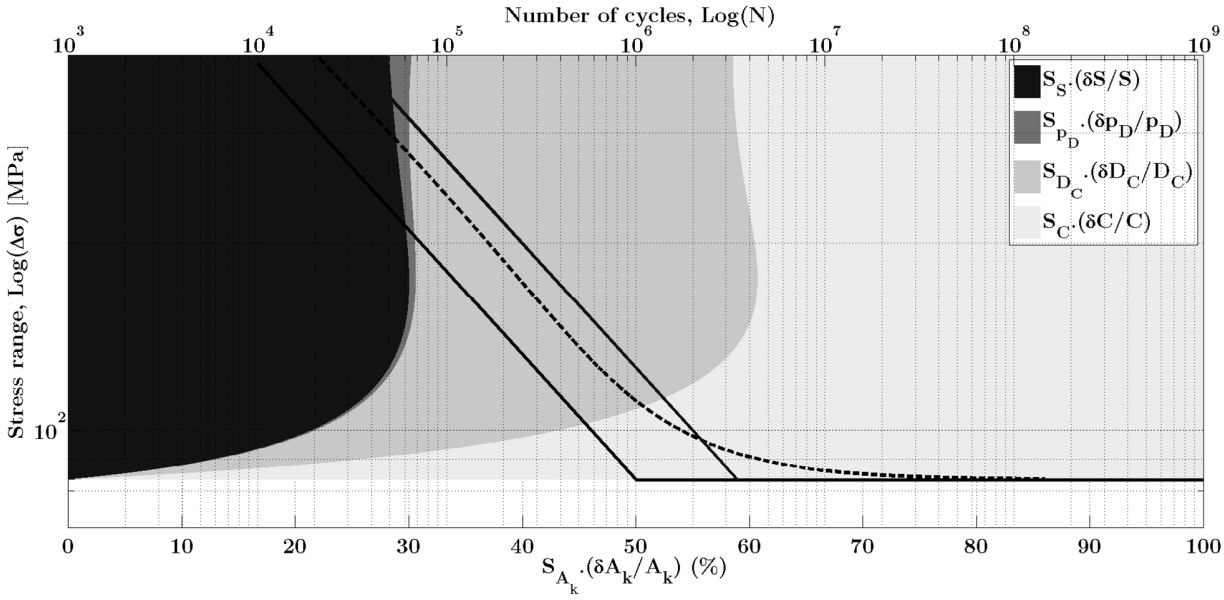

Figure 9: Sensitivity indexes in % (prior)

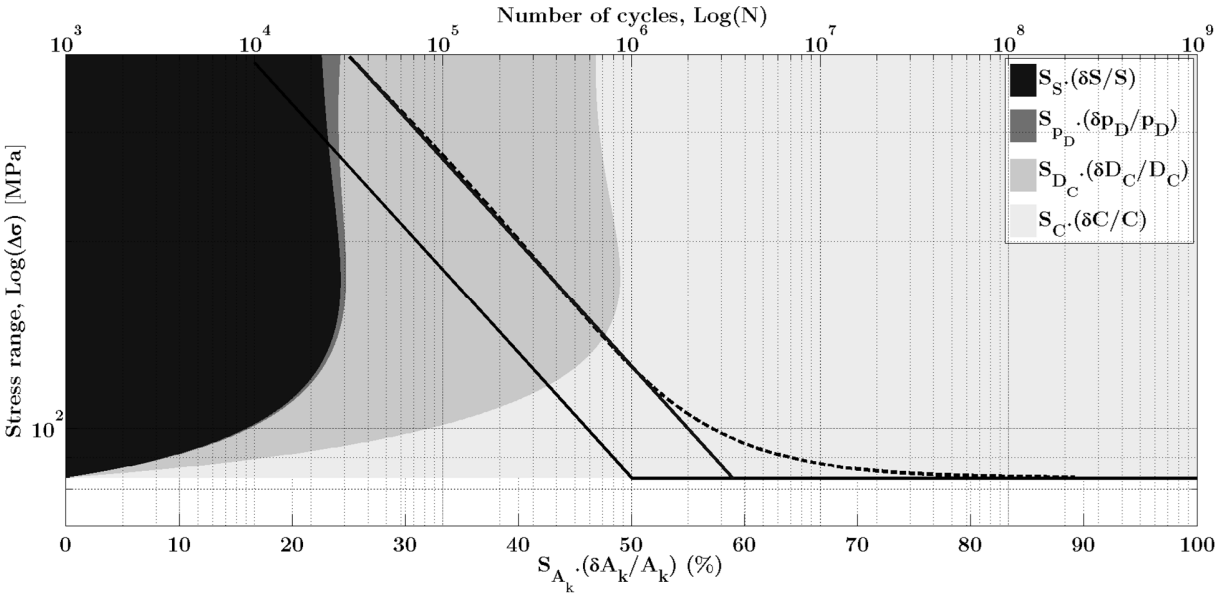

Figure 10: Sensitivity indexes in % (posterior)

	C [MPa]	D_C [-]	p_d [-]	S [MPa]
Ranges of variation	$2 \times 10^6 : 3 \times 10^6$	0 : 0.5	0.1 : 1	0.001 : 1

Table 1: Parameters ranges of variation

Function	Error	Likelihood
Function 1	$e_{ij} = \log\left(N_{exp_i}\right) - \log(N_{model})$	$L = \prod_j^m \prod_i^n \varphi(e_{ij})$
Function 2	$e_j = \frac{1}{n}\sum_i^n \left(\log\left(N_{exp_i}\right) - \log(N_{model})\right)^2$	$L = \prod_j^m \varphi(e_j)$
Function 3	$e_j = \max_i \left\lvert \log\left(N_{exp_i}\right) - \log(N_{model}) \right\rvert$	$L = \prod_j^m \varphi(e_j)$
Function 4	$e_j = \min_i \left\lvert \log\left(N_{exp_i}\right) - \log(N_{model}) \right\rvert$	$L = \prod_j^m \varphi(e_j)$

Table 2: Error and likelihood functions

	C	D_C	p_D	S
CoV	11.51%	35.65%	46.96%	35.76%
Acceptation levels	82.9%	61.1%	84.4%	61.3%

Table 3: Coefficients of variation and acceptation levels

r	C	D_C	p_D	S
C	1	-0.0386	-0.0033	-0.0608
D_C		1	-0.0179	-0.3048
p_D			1	-0.0046
S				1

Table 4: Linear correlation coefficients

	C [MPa]	D_C [-]	p_D [-]	S [MPa]
Ranges of variation	$2 \times 10^6 : 3 \times 10^6$	0 : 0.5	0.1 : 1	0.001 : 1
Mean	2.5×10^6	*0.25*	*0.55*	*0.5005*
CoV	*11.55%*	*57.74%*	*47.24%*	*57.62%*

Table 5: Ranges of variation, means and coefficient of variation of parameters before Bayesian updating

	C [MPa]	D_C [-]	p_D [-]	S [MPa]
Ranges of variation	$2 \times 10^6 : 3 \times 10^6$	0 : 0.5	0.1 : 1	0.001 : 1
Mean	2.509×10^6	*0.3132*	*0.5543*	*0.6223*
C.O.V.	11.51%	35.65%	46.96%	35.76%

Table 6: Ranges of variation, means and coefficient of variation of parameters after Bayesian updating